Journal of Electron Spectroscopy and Related Phenomena, 52 (1990) 661-670
Elsevier Science Publishers B.V., Amsterdam — Printed in The Netherlands

PHOTOELECTRON DYNAMICS OF HI IONIZED BY COHERENT VUV RADIATION

A. Mank, M. Drescher, T. Huth-Fehre, G. Schönhense, N. Böwering and U. Heinzmann

Fakultät für Physik, Universität Bielefeld, D 4800 Bielefeld, F.R.G.

SUMMARY

The asymmetry parameter ß of the photoelectron angular distribution in photoionization of the molecule HI was measured using a tunable coherent VUV source. The target was cooled to a rotational temperature of less than 20 K by a supersonic beam expansion. The data show pronounced resonance structure which is compared to results on a target at nearly room temperature and to an ab-initio calculation by H. Lefebvre-Brion and coworkers.

1. INTRODUCTION

With the development of a coherent VUV radiation source by means of a nonlinear-frequency-mixing technique (1) it is possible to study molecular photoionization governed by one-photon transition selection rules with the necessary high resolution. Results of photoemission yield measurements (2, 3) and first studies of the photoelectron angular distribution (4) have demonstrated the advantages of this light source. The latter study was done on single-photon transitions into the autoionization region between the spin-orbit split $^2\Pi$ ionic ground states of the molecule HI. The molecular beam was prepared close to room temperature; the results were in good overall agreement with previous measurements on HI using synchrotron radiation (5), but revealed more detail due to the higher resolution of the laser based light source. The agreement with an ab-initio calculation (6) was not so good; this could be due to the fact that rotational effects were neglected almost completely in the calculation. This paper reports results of the measurement of the photoelectron angular distribution on a rotationally cooled target (T<20 K) in order to make an approach from the experimental side closer towards the non-rotating case of the calculation.

0368-2048/90/$03.50

2. EXPERIMENTAL

The set-up of the angle resolved photoionization experiment is shown in figure 1. The VUV radiation is generated by non-linear sum-frequency-mixing of linearly polarized pulsed dye-laser radiation in mercury vapor. A detailed description of the radiation source (10^{10} photons per pulse, 11 Hz repetition rate, 5ns pulse length, 0.4 cm^{-1} bandwidth) is given elsewhere (2).

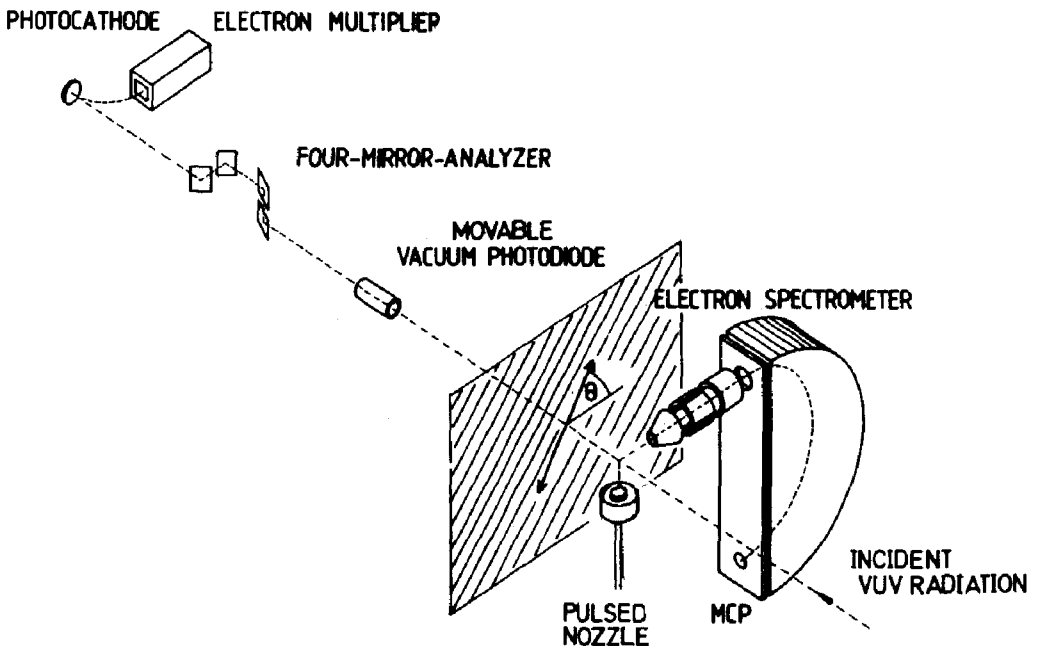

Fig. 1 Experimental set-up for angle resolved photoelectron spectroscopy. The spectrometer analyses electrons ejected perpendicularly to the axis of the incident radiation. The $\vec{E}$-vector of the linear polarization of the VUV radiation can be rotated around the beam axis. The intensity of the VUV is monitored by a vacuum photodiode; alternatively, the polarization can be determined by a four-mirror analyzer.

The VUV radiation crosses a molecular beam from a pulsed nozzle (Lasertechnics LPV with 300μm orifice). The supersonic expansion in the nozzle at a pressure of 150 mbar cools the molecular rotation to below 20 K. The intensity of the VUV is monitored by a vacuum photodiode for normalization of the photoelectron intensity data. The photodiode can be moved out of the beam axis in order to analyze the polarization of the VUV by means of a four-mirror-reflecting analyzer. The polarization of the VUV source was measured to be better than 90 %.

The photoelectron intensity in this geometrical arrangement is proportional to:

$$I(\theta) \propto 1 + \frac{\beta}{4} (1 + 3 P \cos(2\theta)) \qquad (1)$$

where P is the degree of the linear polarization of the incident radiation and θ is the angle between the electric field vector and the momentum of the outgoing photoelectron. The asymmetry parameter β characterizes the deviation of the angular dependence of the electron intensity from isotropy. Equation 1 holds for both partially linearly polarized and elliptically polarized radiation (7). The electric field vector of the linear polarization of the VUV can be rotated by rotating the $\vec{E}$-vector of the visible and ultraviolet dye-laser radiation with a $\lambda/_2$-Fresnel rhomb.
The photoelectrons emitted perpendicularly to the VUV are energy-analyzed in a simulated hemispherical spectrometer (8) and detected by a multichannel plate. A typical photoelectron spectrum is shown in figure 2.

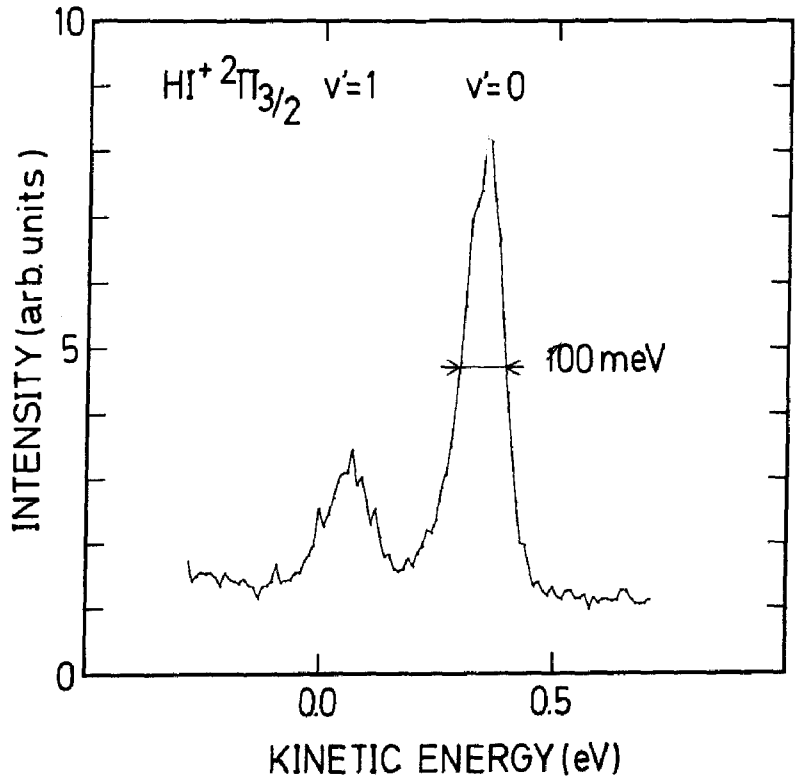

Fig. 2 Photoelectron spectrum of HI at a photon energy of 86650 cm^{-1}. The two peaks correspond to the different vibrational levels of the final ionic state.

The pass energy of the analyzer is set to 3.6 eV giving a resolution (FWHM) of 100 meV. The acceptance angle of the spectrometer is $\Delta\,\theta = \pm 4^{\circ}$. The two peaks in the photoelectron spectrum correspond to the two possible vibrational states of the molecular ion.

In order to check the validity of Equation 1, full angular dependences of the photoelectron intensity were measured by rotating the $\vec{E}$-vector of the VUV. As an example, the results at a photon energy of 86700 cm^{-1} are shown in figure 3.

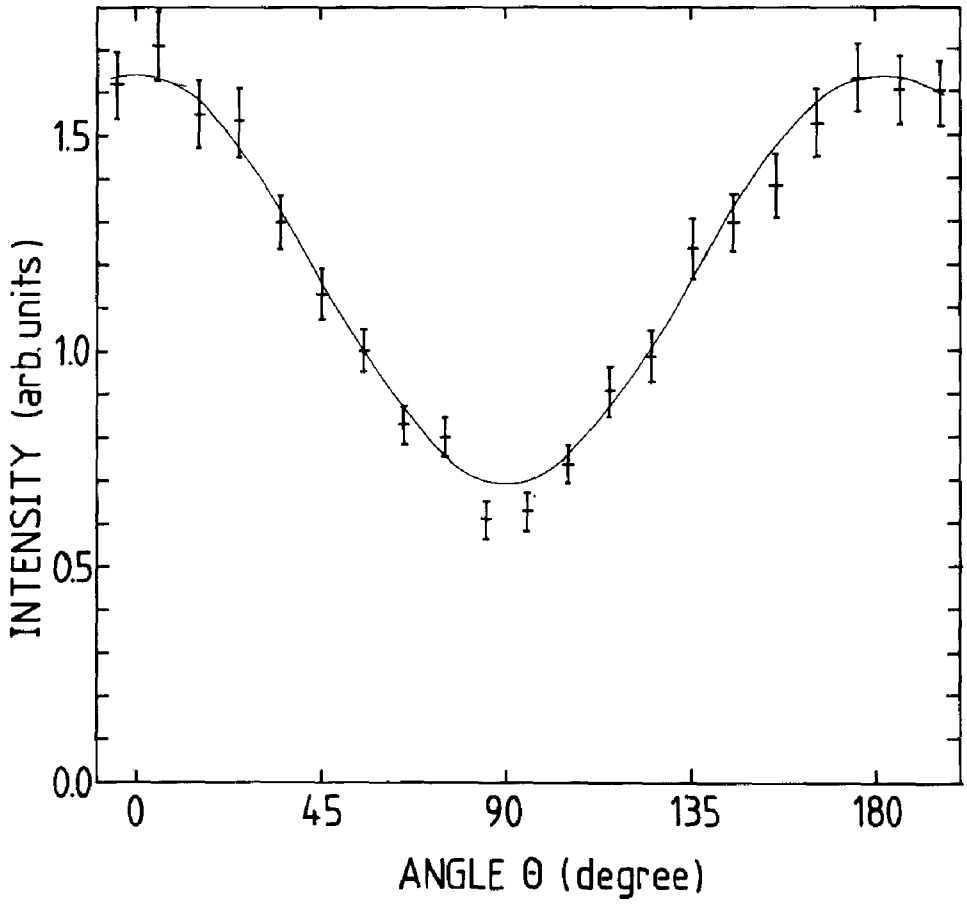

Fig. 3 Angular dependence of the photoelectron intensity at a photon energy of 86700 cm^{-1}. The experimental points are denoted by error bars giving the single statistical error. The full drawn line is a least-squares fit to Eq.1.

The full drawn line (least-squares fit) was obtained with a degree of linear polarization of the VUV of P = 0.94. The fit gives a ß-value of 0.68.

The asymmetry parameters of the angular intensity distribution are obtained from pairs of constant-ionic-state runs with the polarization of the VUV radiation parallel ($\theta = 0^\circ$) and perpendicular ($\theta = 90^\circ$) to the momentum of the electrons accepted by the spectrometer. The asymmetry parameter β can then be determined directly from the ratio R of the intensities $I(0^\circ)/I(90^\circ)$ and P, the degree of the linear polarization, according to:

$$\beta = \frac{4\,(R - 1)}{1 - R + 3\,P\,(R + 1)} \qquad (2)$$

RESULTS AND DISCUSSION

The variation of the photoelectron intensity with the photon energy for the $^2\Pi_{3/2}$ ($v' = 0$) final state of the HI^+ ion are presented in figure 4a. The upper curve gives the intensity with $\theta = 0^\circ$, the lower curve with $\theta = 90^\circ$. The results are shown with error bars representing the single statistical error. Each data point is the sum of several runs accumulated. The resulting asymmetry parameter β is shown in figure 4b. The experimental points are denoted by error bars containing the errors of the intensities and the uncertainty of the VUV polarization.

The resonance structure observed results from the ($n_{eff} = 7$) members of Rydberg-series of the configuration HI $(5\pi)^3$ $nl\lambda$ converging to the ionization limit of the $^2\Pi_{1/2}$ ($v' = 0$) ionic state at 89125 cm^{-1} (3). The Rydberg states autoionize via spin-orbit interaction into the continuum leaving the ion in the $^2\Pi_{3/2}$ ($v' = 0$) ground state. The spectrum is dominated by a broad resonance at 86700 cm^{-1} and shows many smaller structures.

To understand the main features of the spectrum we can make a comparison with the photoionization of xenon, the corresponding isoelectronic atom. In xenon, the same autoionization process occurs in the photoionization of the 5p shell. Angular momentum selection rules in atoms lead to two Rydberg-series: ns, nd. In xenon, the nd-series exhibits broad resonances on which the ns-series is superimposed. Across the broad nd-resonances, a β-value of $\approx 0{,}7$ was measured, with β approaching $\approx -0{,}7$ at the minimum of the Fano-profile (9).

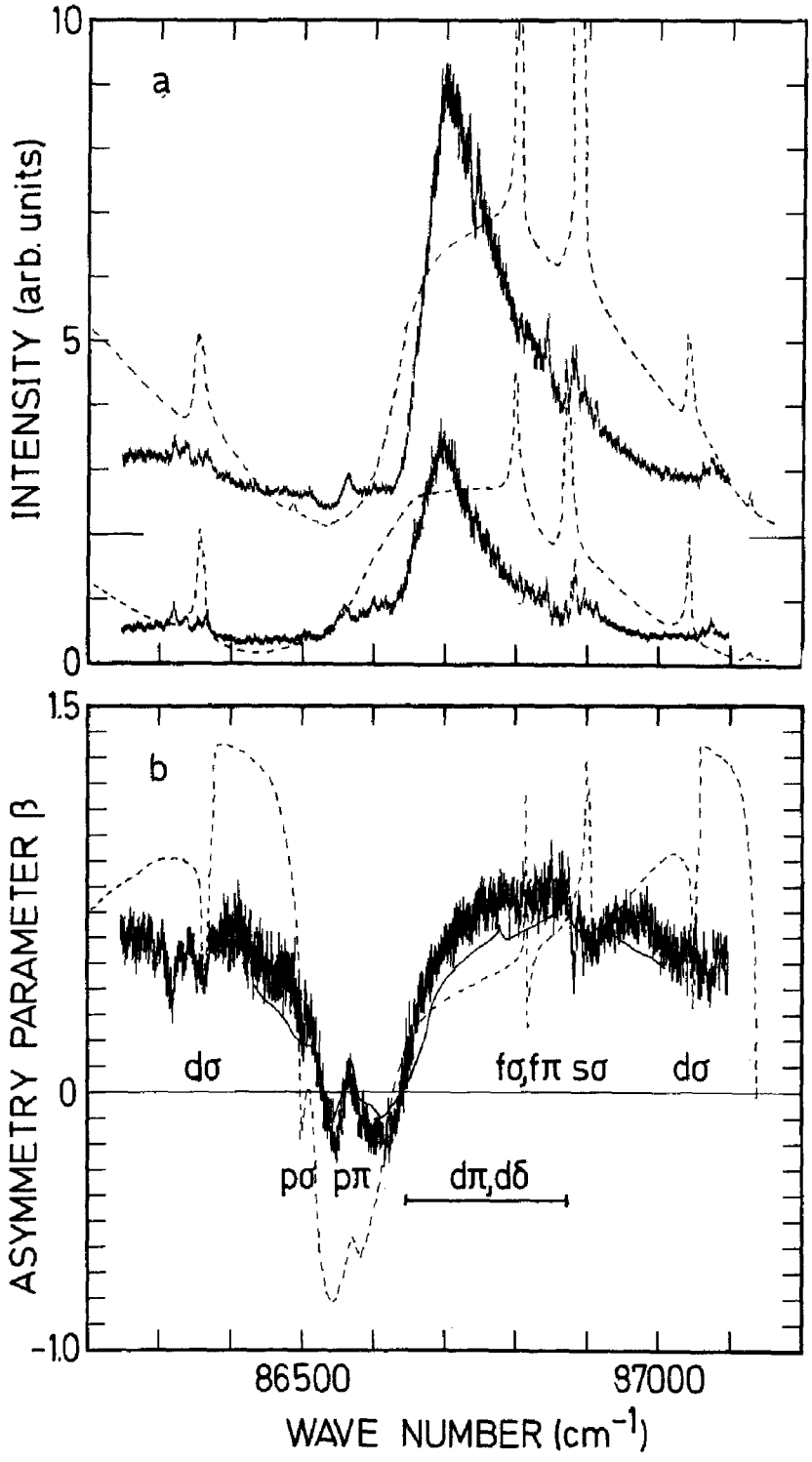

Fig. 4 Results for intensity and asymmetry parameter ß. Figure 4a shows the electron intensities for $\Theta = 0^{\circ}$ (upper plot) and $\Theta = 90^{\circ}$ (lower plot). The zero line for the upper plot is denoted by the longer bar. The resulting asymmetry parameter ß is given in figure 4b. The experimental data are represented by their error bars. The dashed lines are the results of an ab-initio calculation (6), the classification of the resonances is also taken from this reference. The full line shows the results of a measurement on a target at nearly room temperature (4).

Due to the reduced symmetry of the molecule, the angular momentum of the electron l is no longer a good quantum number, only its projection λ onto the molecular axis is valid. The reduced symmetry gives different angular momentum selection rules leading to more transitions. By comparison with xenon, the broad feature in Fig. 4b can be assigned to a $\pi \rightarrow d\delta$,$d\pi$ transition. The complex structure at around 86900 cm^{-1} (see also Fig. 4a) should be assigned to a $\pi \rightarrow s\sigma$ transition. The angular distribution asymmetry parameter across the broad resonance exhibits similar behaviour as in xenon, although the minimum of the profile is not as pronounced. At the position of the possible $\pi \rightarrow s\sigma$ transition, several small resonance structures are observed in the ß-parameter.

The most pronounced feature that does occur in HI but not in xenon is the resonance at 86570 cm^{-1} superimposed onto the minimum in the asymmetry parameter. Further structure can be seen in Fig. 4 between 86300 cm^{-1} and 86400 cm^{-1} and around 87080 cm^{-1}. In the intensity spectra, additional resonances can be seen around 86740 cm^{-1} without corresponding structure in the asymmetry parameter. Apart from the transitions that can be found correspondingly in xenon, the following molecular transitions are possible: $\pi \rightarrow p\sigma$, $p\pi$, $d\sigma$, $f\sigma$, $f\pi$ or even higher angular momentum states.

All the transitions should exhibit rotational fine structure. At a rotational temperature of less than 20 K, only the substates with J = 0, J = 1 and J = 2 of the molecular ground state are populated significantly with a distribution of roughly 35 % : 45 % : 15 %, respectively. The intermediate states are either Σ ($\pi \rightarrow \pi$) or Π ($\pi \rightarrow \sigma$, $\pi \rightarrow \delta$). For a Σ-state, the following lines might be expected: a weak P(2), a P(1), no Q-branch, a R(0), a R(1) and a weak R(2). For a Π-state, one expects: a weak P(2), no P(1), a Q-branch with Q(1) and a weak Q(2), a R(0), a R(1), and a weak R(2). The rotational constant for the ground state of HI is B_0 = 6.5 cm^{-1} (10) and since the potential curve for the $^2\Pi$ ionic ground state is very similar to the neutral ground state one can expect an average spacing of the rotational lines of 13 cm^{-1}. Therefore, a Σ state arising from a $\pi \rightarrow \pi$ transition should show 3 lines, two at a distance of 13 cm^{-1} and a third 26 cm^{-1} to lower energies because of the missing Q-branch. A Π-state, arising from

$\pi \rightarrow \sigma$, $\pi \rightarrow \delta$ transitions should show 3 lines with a spacing of 13 cm^{-1} each. However, such a simple rotational distribution can not be found anywhere in the spectrum.

In the attempt to assign the different transitions, we used an ab-initio MQDT calculation of the autoionizing Rydberg-series by Lefebvre-Brion et al. (6) as a guideline. The calculation was performed not only for the cross section but also for the other dynamical parameters of the photoionization process (asymmetry and spin-polarization parameters) for the (n_{eff} = 6) members of the Rydberg series. We have scaled the results to (n_{eff} = 7) in order to compare the calculation with our experimental values. Furthermore, we evaluated the intensities for $\theta = 90^{\circ}$ and $\theta = 0^{\circ}$ from the results of the calculation of the total cross section and the ß-asymmetry parameter. The dashed lines in figure 4 show the prediction of the calculation; it was shifted by 60 cm^{-1} to lower energies in order to achieve best agreement at the resonance positions.

The calculation shows a reasonable agreement with our measurements. The calculation does not show rotational lines but a single transition since no rotational distribution of the ground state was taken into account. The behaviour of the asymmetry parameter across the broad resonance is reproduced quite closely. It also accounts for the pπ resonance at 86570 cm^{-1} though the minimum is deeper than the experimental results show. Several problems do occur, however. The intensity in the $\pi \rightarrow d\delta$, dπ transition is too high compared to the other transitions. Only part of this problem can be attributed to the fact, that the intensity of the sharp resonances has to be distributed over the rotational lines, whereas the broad resonance has a width that includes all rotational lines. Due to the width of this transition no fine structure should be seen - but around 86740 cm^{-1}, there is fine structure in the experimental intensity data, that has the correct spacing for a $\pi \rightarrow d\delta$ rotational transition. It is not possible to assign rotational lines of the $\pi \rightarrow p\pi$ transition, since only one line can be seen clearly and the other two should have nearly the same intensity.

The distance between the sσ and the fσ, fπ resonance is smaller than in the calculation, the best assignment for the structure

between 86800 cm^{-1} and 86900 cm^{-1} being a mixture of these states. If we attempt to assign rotational lines, no unambiguous assignment is possible. Furthermore, the behaviour of the ß-parameter in this region is not as it was expected from the calculation.

The assignment of the dσ-resonances (n_{eff} = 6 near 86325 cm^{-1}, n_{eff} = 7 at 87080 cm^{-1}) is supported by the calculation showing agreement with the experimental values of the ß-parameter. From the different shapes of the two resonances we deduce that one of them is pertubated by another, so far unknown state. Since the structure between 86300 cm^{-1} and 86400 cm^{-1} cannot be fitted into a rotational progression, this should be the pertubated one. The assignment of the resonance at 86325 cm^{-1} as a dσ-transition is supported by results of recent measurements of the spin-polarization parameter A (11) yielding the calculated behaviour at this resonance. From the ß-parameter data alone, the structure at 86360 cm^{-1} could also be the dσ-resonance. For the pσ-transition, no clear assignment can be made.

For comparison, experimental results of the asymmetry parameter ß on a target at nearly room temperature (4) are shown as a solid line in figure 4b. The overall shape across the dπ, dδ and pπ transition is the same as for the cold HI beam, only the structure due to the fσ, fπ and sσ transitions cannot be seen as clearly. This can be explained since the effect of rotational cooling should be stronger with sharp resonances than with broad ones.

Experimental results on the dynamics of molecular autoionization on rotationally cooled HI molecules with high resolution were presented. The results show fine structure due to molecular rotation but the complexity of the problem has made an unambiguous assignment so far impossible. Further work on the spin-polarization of photoelectrons may help to identify the assignment of the rotational fine structure. Theoretical calculations of the dynamical parameters in the photoionization of HI show reasonable agreement, but have to be improved to reproduce the details of the experimental data more closely. A dependence of the experimental data on the rotational temperature of the target could only be found in the fine structure of the data; the overall

shape of the angular distribution asymmetry parameter remains unchanged.

We thank R. Wallenstein, H. Lefebvre-Brion and G. Raseev for valuable discussions. This work was supported by the Deutsche Forschungsgemeinschaft (SFB 216) and the European Commission.

REFERENCES

/1/ R. Hilbig and R. Wallenstein, IEEE Journal of Quantum Electronics, QE-19 (1983), 1759-1770.
/2/ T. Huth, A. Mank, N. Böwering, G. Schönhense, R. Wallenstein and U. Heinzmann in: H.B. Gilbody, W.R. Newell, F.H. Read, and A.C.H. Smith (Eds.), Electronic and Atomic Collisions, Elsevier, London, New York (1988), p. 607-612.
/3/ D.J. Hart and J.W. Hepburn, Chem. Phys. 129 (1989) 51-64.
/4/ A. Mank, M. Drescher, T. Huth-Fehre, G. Schönhense, N. Böwering and U. Heinzmann, submitted to J. Phys. B.
/5/ T.A. Carlson, P. Gerard, M.O. Krause, G. von Wald, J.W. Taylor and F.A. Grimm, J. Chem. Phys. 84 (1986), 4755-4759.
/6/ H. Lefebvre-Brion, A. Giusti-Suzor and G. Raseev, J. Chem. Phys. 83 (1985) 1557-1566.
/7/ V. Schmidt, Phys. Lett. 45A (1973) 63-64.
/8/ K. Jost, J. Phys. E12 (1979) 1006-1012.
/9/ J.A.R. Samson and J.L. Gardner, Phys. Rev. Lett. 31(1973) 1327-1330.
/10/ S.G. Tilford, M.L. Ginter and A.M. Bass, J. Mol. Spectroscopy 34(1970) 327-340 ,57 (1975) 271-283.
/11/ T. Huth-Fehre, A. Mank, M. Drescher, N. Böwering and U. Heinzmann, submitted to Physica Scripta.